Clim. Past Discuss., 9, 2681–2715, 2013
www.clim-past-discuss.net/9/2681/2013/
doi:10.5194/cpd-9-2681-2013
© Author(s) 2013. CC Attribution 3.0 License.

Climate of the Past Discussions
Open Access

This discussion paper is/has been under review for the journal Climate of the Past (CP).
Please refer to the corresponding final paper in CP if available.

Siple Dome shallow ice cores: a study in coastal dome microclimatology

T. R. Jones[1], **J. W. C. White**[1], **and T. Popp**[2]

[1]Institute of Arctic and Alpine Research, University of Colorado, Boulder, Colorado, USA
[2]Centre for Ice and Climate, Niels Bohr Institute, University of Copenhagen, Copenhagen, Denmark

Received: 19 April 2013 – Accepted: 27 April 2013 – Published: 24 May 2013

Correspondence to: T. R. Jones (tyler.jones@colorado.edu)

Published by Copernicus Publications on behalf of the European Geosciences Union.

Abstract

Ice cores at Siple Dome, West Antarctic receive the majority of their precipitation from Pacific Ocean moisture sources. Pacific climate patterns, particularly in response to the El Niño-Southern Oscillation, affect local temperature, atmospheric circulation, snow accumulation, and water isotope signals at Siple Dome. We examined borehole temperatures, accumulation, and water isotopes from a number of shallow ice cores recovered from a 60 km north–south transect of the Dome. The data (with coverage from 1920–1995) reveal a microclimate heavily influenced by ENSO and the location of the Amundsen Sea Low Pressure Area. The Dome Summit and Pacific Flank respond to La Niña conditions by warming, increased isotope ratios, higher deuterium excess, and increased snowfall. The Inland Flank responds to El Niño conditions and cold interior air masses by cooling, decreased isotope ratios, lower deuterium excess, and decreased snowfall. ENSO-type spectral signatures (2–7 yr) are present in all water isotope records, but are not similar in their power structures. A longer 300 yr wavelet analysis record from the Dome Summit shows a late 19th-century climate shift similar to that seen in South Pacific coral isotope records. Our analyses suggest that while an ENSO signal is evident at Siple Dome, the microclimate effect makes climate reconstruction problematic, a conclusion which should be considered at other West Antarctic coastal dome locations.

1 Introduction

The Siple Dome ice core was drilled as part of the West Antarctic Ice Sheet (WAIS) initiative managed by the National Science Foundation (NSF) Office of Polar Programs (OPP). Originally one of two deep WAIS initiative ice cores (the other being the inland and more elevated WAIS Divide), Siple Dome's coastal location in the Pacific sector of Antarctica was selected in part to study climate signals such as the El Niño Southern Oscillation (ENSO). In this study, we evaluate a series of shallow ice cores to determine

CPD
9, 2681–2715, 2013

the feasibility of long-term tropical climate reconstruction using coastal ice core sites in West Antarctica (WA).

1.1 Antarctic ENSO teleconnection

ENSO is a large-scale ocean-atmosphere climate phenomenon linked to the intermittent warming (El Niño phase) and cooling (La Niña phase) of the central and east central equatorial Pacific Ocean (Trenberth and Hoar, 1997). ENSO is characterized by year-to-year spatial variations in sea surface temperatures, convective rainfall, surface air pressure, and atmospheric circulation, the effects of which not only influence the equatorial Pacific, but also influence worldwide weather patterns via teleconnection (Diaz et al., 2001).

Research has shown that teleconnected ENSO climate signals are pervasive across the Antarctic continent (Turner, 2004). In WA, ENSO has been shown to affect atmospheric circulation, local temperature, and snow accumulation (Delaygue et al., 2000; Bromwich et al., 2004; Guo et al., 2004; Schneider et al., 2004) through modulation of the Amundsen Sea Low Pressure Area (ASL) (Cullather et al., 1996; Bromwich et al., 2000; Bertler et al., 2004; Guo et al., 2004). The exact location and phasing of the ASL in relation to ENSO is not fully characterized and has been the topic of numerous studies (Fig. 1). Bertler et al. (2006) show that during La Niña events, the ASL is centered in the Ross Sea, directly off the Ross Ice Shelf, and transports a relatively warm air mass into the Ross Sea region of WA. Similar findings have shown that heat and moisture transport into WA is most effective when the ASL is centered over the Ross Sea (Nicolas and Bromwich, 2011). During El Niño events, the effect of the ASL on Siple Dome climate is less clear. Bertler et al. (2006) show that the ASL shifts eastwards towards the Amundsen Sea and transports an even warmer air mass into Marie Byrd Land, which cools significantly over inland WA, eventually flowing downslope into the vicinity of Siple Dome. However, Markle et al. (2012) show that the ASL is shifted much more westward into the Ross Sea (in disagreement with the Bertler study). In either

CPD
9, 2681–2715, 2013

case, ASL-El Niño events have been linked to katabatic surges over inland WA and across the Ross Ice Shelf (Bromwich et al., 1993).

Numerous studies have determined that the ASL strengthens during La Niña events and weakens during El Niño events, resulting in widespread climatic anomalies (Cullather et al., 1996; Bromwich et al., 2000; Meyerson et al., 2002; Carleton, 2003; Bertler et al., 2006). The Bertler et al. (2006) study has shown that the ASL causes sea surface temperature (SST) anomalies of ∼ 0.5 °C cooling during La Niña events and ∼ 0.5 °C warming during El Niño events in the Amundsen and Ross Seas. A stronger but opposing atmospheric ASL-ENSO effect causes up to ∼ 15 °C near surface temperature anomalies in the eastern Ross Sea, resulting in a net cooling during El Niño events and a net warming during La Niña events. Siple Dome is centrally located to experience both ASL-ENSO modes.

1.2 Siple Dome shallow ice cores

We analyzed water isotopes, borehole temperatures, and accumulation rates from a series of seven shallow ice cores (B–H) spanning a 60 km north-south transect of Siple Dome. Our measurements span the years 1920–1995 for Cores C–H, as well as the years 1657–1995 for Core B. First, we seek to characterize the ENSO teleconnection in water isotopes of Core B (located in the same location as the Siple Dome deep ice core) using time series re-dating techniques, Multi-Taper Method spectral analysis, and Continuous Wavelet Transform spectral analysis. Our focus then shifts to the overall climate signal at Siple Dome, including ASL-ENSO driven effects. We base our study on the following questions: (1) To what extent is ENSO evident at Siple Dome? (2) How does the ASL-ENSO system affect the coherence of climate signals recorded in the shallow ice cores? (3) How reliable are ENSO reconstructions using coastal dome ice core sites in West Antarctica? We find that while an ENSO signal is identifiable at Siple Dome, a microclimate effect related to the ASL-ENSO dynamic makes meaningful ENSO reconstructions difficult.

CPD
9, 2681–2715, 2013

2 Site description

Siple Dome is located in WA on the Siple Coast at approximately 81°40′ S and 148°49′ W. The Siple Coast contains five major ice streams (A–E), which drain part of the West Antarctic Ice Shelf "WAIS" and is immediately adjacent to the Ross Ice Shelf. Siple Dome is located between ice streams C and D. Figure 2 shows the ice core locations and elevations used in the present study. Drill sites include two cores on the north flank of the Dome facing the Pacific Ocean (E and G), three cores from the summit of the Dome (B, C and D), and two cores on the south flank of the Dome facing inland (H and F). Table 1 summarizes the details for each ice core location.

3 Methods

3.1 Water isotopes

To study the ASL-ENSO dynamic at Siple Dome, we utilize water isotopes as a climate tracer. Isotopic composition is expressed in delta notation (δ) relative to VSMOW using the following equation:

$$\delta_{\text{sample}} = [(R_{\text{sample}}/R_{\text{VSMOW}}) - 1] \times 1000 \quad (1)$$

where R is the isotopic ratio $^{18}O/^{16}O$ or D/H in the sample or VSMOW. We utilize a Rayleigh model to characterize condensation in open systems, where the isotopic composition of precipitation is correlated with cloud temperature (Dansgaard, 1964). The correlation between δD and surface temperature has been empirically defined as:

$$\delta D = 5.6 T_{\text{average}} - 100$$

where T_{average} is the mean annual surface temperature at the collection site. In cold regions, the fractionation between water vapor and precipitation is strongest, such that

CPD
9, 2681–2715, 2013

δD and δ^{18}O have a higher rate of depletion at high latitudes. More recent studies from Antarctica show the slope is as high as 6.34 ‰ ± 0.09 ‰ per 1 °C (Masson-Delmotte et al., 2008), a value which we use in this study.

Deuterium excess (XS), a second order parameter, is defined as:

$$XS = \delta D - 8\delta^{18}O \quad (2)$$

where XS in water vapor depends on both phase changes of water under equilibrium conditions and a kinetic effect resulting from different diffusivities of water molecules. For example, $D^1H^{16}O$ (mass of 19) will diffuse faster than $^1H^1H^{18}O$ (mass of 20), resulting in higher XS during deviation from equilibrium conditions. The initial isotope concentration in an air parcel will have a XS value that is a function of sea surface temperature, relative humidity and wind speed (Jouzel and Merlivat, 1984). Sea surface temperature has been shown to be the primary determinant of XS values in Antarctic snow (Petit et al., 1991).

A number of factors are known to affect Antarctic δ values, including: (1) additional poleward evaporation and enrichment of isotopic signals originating at lower latitudes, which limits variability of δ over the ice sheets (Hendricks et al., 2000; Noone and Simmonds, 2002); (2) katabatic winds that transport isotopically depleted inland snow towards the coast (Bromwich et al., 1993); (3) additional kinetic isotopic fractionation during condensation of snow crystals in supersaturated air masses (Jouzel and Merlivat, 1984); (4) changes in temperature and/or location of the primary moisture source region (Kavanaugh and Cuffey, 2003); and (5) changes in the strength and/or height of the inversion layer (discussed in Blunier et al., 1998 and Kavanaugh and Cuffey, 2003). Despite the aforementioned factors, Antarctic δ values have been shown to reliably capture most temperature variations within (−)10 to (+)30 % (Jouzel et al., 2003). In this study, as a first order assumption, isotopes at Siple Dome are assumed to detect local temperature signals related to the region's mean annual climate.

CPD
9, 2681–2715, 2013

3.2 Field and laboratory

Siple Dome shallow cores B–H were drilled in the 1996–1997 field season to explore the spatial variability of various climatic and meteorological signals such as ENSO. Following extraction, these cores were analyzed for stable hydrogen and oxygen isotopes of water (Steig and White, 2003), and a depth-age dating scheme was developed based upon visual stratigraphy (Alley, 2003). The ice was sampled at the National Ice Core Laboratory (NICL) in Lakewood, Colorado and isotopically analyzed at the Institute of Arctic and Alpine Research (INSTAAR) Stable Isotope Lab (SIL) at the University of Colorado.

The SIL analyzed both δD and δ^{18}O values of water using SIRA Prism Micromass mass spectrometers. Hydrogen isotopic ratios were determined using an automated direct injection uranium reduction system (Vaughn et al., 1998) with an uncertainty of ±1.0 ‰. Oxygen isotopic ratios were determined with an automated version of the traditional CO_2/H_2O equilibration method (Epstein and Mayeda, 1953) with an uncertainty of ±0.1 ‰. The shallow ice cores were sampled at 5 cm increments, yielding sub-annual temporal resolution (approximately 2–6 samples per year) until at least the year 1920. High temporal resolution data for Core B extends as far back as 1657.

In this study, we employ a number of field and laboratory measurements for interpretation of the isotopic record. 20 m borehole temperatures taken by Clow (1996) constrain the mean annual temperature and local climate at Siple Dome. At 20 m, the borehole temperatures are not influenced by seasonal fluctuations in surface temperature. Borehole temperature data is not available for Core E on the North flank (Pacific facing), so we calculate this value using a range of temperature estimates. Mass accumulation rates were determined from depth-age dating schemes and a 3rd order polynomial fit of 1 m density measurements (Lamorey, 2003).

CPD
9, 2681–2715, 2013

3.3 Data and procedures

We compare δD to the Southern Oscillation Index (SOI), which is a proxy for atmospheric ENSO pressure anomalies, using Spectral Analysis and time-series dating techniques (explained in subsequent paragraphs). The SOI captures ENSO processes by measuring departures from normal in the surface air pressure difference occurring between the western and eastern tropical Pacific, or more specifically, between Tahiti, French Polynesia and Darwin, Australia. The SOI provides a record of ENSO dating back to 1876, but observations are most accurate after 1950 due to better measurement techniques. We use December-January-February-March (DJFM) averages of the SOI to best capture ENSO, an austral summer phenomenon. δD isotopic measurements were re-dated to align with the SOI within annual layer counting dating uncertainty to test for coherency amongst the shallow ice core data sets (but not to reconstruct ENSO itself). We place emphasis on the δD of Core B (δD_B), the longest shallow ice core (dating to 1657), which was drilled in the same location as the deep Siple Dome ice core.

Spectral analysis of the δD_B record was performed with Kspectra, a software program used to interpret time series with low signal to noise ratios. The Multi-Taper Method (MTM) utilized by Kspectra is non-parametric and provides a means for spectral estimation and signal reconstruction (Thomson, 1982; Percival and Walden, 1993; Ghil et al., 2002). Continuous Wavelet Transform (CWT) was used to interpret local variations in the power spectrum of the δD_B time series. CWT changes a one-dimensional time series into time-frequency space, creating a two dimensional image of modal variability through time (Torrence and Compo, 1998). Both the spectral and wavelet power spectrums are based on a Morlet function and a red noise background spectrum.

The relatively warmer temperatures and lower accumulation rates at Siple Dome compared to other Antarctic ice core sites are more conducive to diffusion of water molecules in the firn. Isotopic diffusion is capable of eroding spectral power at high frequencies (low periodicities), causing the loss of seasonal and yearly isotopic signals

CPD
9, 2681–2715, 2013

in the ice core record. A full analysis of isotopic diffusion in polar firn can be found in Cuffey and Steig (1998).

4 Results

4.1 ENSO signals

MTM spectral analysis of the SOI record and shallow ice core δD records reveals typical ENSO periodicities (2–7 yr range), in varying degrees, from 1920–1995 (Fig. 3). During this time period, the SOI spectral band includes 95 % statistically significant periodicities ranging from 2.3–2.4, 3.6, and 4.5–6.1 yr, with the strongest spectral power in the 4.5 yr periodicity. The higher 4.5–6.1 yr SOI band is well represented in every core site, except Core G, which has lower power in this band. The 2.3–2.4 and 3.6 yr SOI bands are well represented in all cores, except for Core G and Core F, which have less power in the 3.6 yr SOI band. Among all shallow cores, the significant periodicities of Core H (Inland) extend to 11.1 yr, whereas Core G (Pacific) only extends to 4.7 yr. The most persistent signal is evident in the δD_B record, which has significant power in almost all classical ENSO periodicities in the 2–7 yr range between 1920–1995.

At longer time scales (1657–1995), CWT shows a distinct shift in the δD_B power spectrum (Fig. 4). Prior to the late 19th century to early 20th century, scattered bi-decadal to decadal periodicities are evident in δD_B, whereas periodicities after this transition are more intensely grouped and decrease to 2–3 yr at the end of the 20th century. Similar to Siple Dome, a systematic climate shift is also seen in ENSO-correlated Pacific Ocean coral isotope records. Urvina Bay $\delta^{18}O$ coral data (Galapagos Islands, eastern tropical Pacific Ocean) records a shift to shorter periodicities in the middle to late 19th century, potentially caused by long-term solar cycles operating at classical ENSO and decadal scale periods (Dunbar et al., 1994). Studies from Maiana Atoll $\delta^{18}O$ coral records (central tropical Pacific Ocean) show prominent decadal variability during cooler and drier background conditions in the mid-late 19th century, and warmer

CPD
9, 2681–2715, 2013

and wetter conditions with shorter period variability in the 20th century (Urban et al., 2000). These distinctive shifts in tropical coral isotopes, as well as Siple Dome water isotopes, suggest that large-scale ENSO reorganizations have far-reaching effects capable of influencing climate in WA, thereby affecting ice core records.

When δD_B is re-dated to the DJFM SOI from 1876–1995, an inverse relationship is evident (Fig. 5). That is, during ENSO cool events (La Niña), δD_B values are more enriched (warmer signal), and during ENSO warm events (El Niño), δD_B values are more depleted (colder signal). This inverse relationship suggests that Siple Dome water isotopes are recording the opposite temperature signal as tropical ENSO SSTs. All re-dated (within layer counted uncertainty) shallow core δD records are shown in Fig. 6. While similarities exist amongst the re-dated δD records over various time scales, there is no general agreement between the water isotope records on the Pacific Flank, Dome Summit, and Inland Flank. The most pronounced difference in re-dated records occurs between δD_E (Pacific) and δD_F (Inland).

4.2 Local climate at Siple Dome from 1920–1995

Shallow borehole temperature observations at 20 m depth reveal two distinct temperature gradients across Siple Dome, including a cold regime on the Inland Flank and a warmer regime on the Dome Summit and Pacific Flank (Fig. 7). The borehole temperature at G2 (Pacific) relative to L (Dome) falls within 0.13 °C from that expected by the local adiabat (defined as 0.82 °C atmospheric cooling per 100 m of elevation gain). No borehole temperature was taken at Core E (Pacific), so the maximum extent of warming towards the Pacific is unknown. The Inland Flank adheres to an adiabatic trend ~1–2 °C colder than the Dome Summit and Pacific Flank. The borehole temperature at J (Inland) relative to H (Inland) is colder by 0.05 °C than would be predicted by the local adiabat. Overall, the warmest and coldest parts of the Dome relative to elevation are 30 km towards the Pacific and 30 km inland. All local climate information (borehole temperatures, accumulation, and water isotopes) is shown in Table 2.

CPD
9, 2681–2715, 2013

Mass accumulation and standard deviation of water isotopes are calculated for all shallow cores (Fig. 8). Mass accumulation is a direct measure of the amount of precipitation an ice core site experiences, while the standard deviation of ice core water isotopes is a useful measure of climate signal strength. The path atmospheric water vapor takes before deposition at an ice core site will influence how pronounced seasonal and yearly oscillations are in the isotopic record. At an ice core location with relatively high standard deviation, it can be assumed that a parcel of water vapor experienced less depletion events, and/or originated in an area of more pronounced climate variability than an ice core location with low standard deviation. In general (but not always), mass accumulation and standard deviation of water molecules will covary at an ice core site, where increased accumulation leads to a more variable water isotope signal.

Mass accumulation is greatest at Core G (Pacific), and decreases to the Inland Flank, with the lowest values at Core F (Inland). Although Core E (Pacific) is closest to the ocean and should have a maximum mass accumulation value, it is instead similar to values on the Dome Summit. One possibility is that the area around Core E (Pacific) is too warm for some austral summer precipitation events, and through orographic uplift and cooling of air masses, precipitation events instead occur at higher elevations. A second possibility is that an inversion layer forms during certain parts of the year at Siple Dome, which tends to cap air masses, and eventual precipitation, at elevations above Core E (Pacific). A final possibility is that surface winds move snow after deposition, producing uneven loading due to Dome topography.

The δD standard deviation is highest at Core E (Pacific) and decreases to the Inland Flank, with the lowest value at Core F (Inland). Core B (Dome) standard deviation falls in the middle of Core E (Pacific) and Core F (Inland). The decreasing trend in standard deviation from the Pacific to Inland side is best explained by the location of the ASL in relation to Siple Dome. During La Niña, the ASL is centered near Siple Dome in the Ross Sea, creating a relatively direct ocean-land moisture source connection. For a parcel of water vapor traveling from moisture source to deposition, the direct connection will promote less isotope depletion events, a stronger climate signal, and

CPD
9, 2681–2715, 2013

thus higher standard deviations. During El Niño, the ASL is centered away from Siple Dome in the Amundsen Sea, creating a relatively indirect transport path over Marie Byrd Land. For a parcel of water vapor traveling from moisture source to deposition, the indirect and inland connection will promote more isotope depletion events, a dampened isotopic signal, and thus lower standard deviations. Overall, the difference in water vapor paths causes a more pronounced isotopic signal on the Pacific Flank, whereas the Inland Flank shows a diminished isotopic signal.

4.3 Modeling the isotopic variability

We relate temperature to isotopes using an Antarctic correlation between δD and surface temperature of 6.34 ‰ ± 0.09 ‰ per 1 °C (Masson-Delmotte et al., 2008) (Fig. 9). We assume Core E (Pacific) is the first shallow core to receive moisture because it is closest to the Pacific Ocean. Since no borehole measurement was taken in the vicinity of Core E, a range of temperature estimates (−23.23 to −22.28 °C) are used corresponding to an adiabatic lapse rate of 0.82 °C/100 m (Shimizu, 1964) generated from Borehole G2 (Pacific) and a temperature trend of 0.013 °C km^{-1} between Borehole G2 (Pacific) and Borehole L (Dome). A "theoretical isotope scenario" predicts ice core isotopic values as if moisture was converging on Siple Dome uniformly from both the Pacific and Inland sides. The theoretical scenario serves to offer comparison for the observed effects of the ASL-ENSO system.

Actual measured isotope values show that the heaviest δD values (warm signal) occur at Core E (Pacific), and the lightest δD values (cold signal) occur at Core F (Inland). The temperature difference range between Borehole L (Dome) and Core E (Pacific) is estimated to be 1.89 to 2.84 °C, which corresponds to δD expected isotope depletions on the Dome Summit of 12.0–18.0 ‰, respectively. However, the actual measured difference between Core E (Pacific) and Core B (Dome) is only 3.2 ‰, showing a heavy isotope anomaly on the Dome Summit. One explanation for this occurrence is that temperatures at Core E (Pacific) are at times too warm during the austral summer to produce snow, causing some air masses to bypass Core E (Pacific) and deposit

CPD
9, 2681–2715, 2013

isotopically heavy moisture on the Dome Summit. This explanation is supported by our observation of similar mass accumulation rates between Core E (Pacific) and Core B (Dome). We suggest that while Core E (Pacific) would be expected to have the highest accumulation rate due to its proximity to the ocean, it misses some moisture events, which instead fall at higher elevations causing discrepancies in accumulation rates and δD values.

Water isotope values at Core F (Inland) are too light isotopically compared to Core B (Dome) by −18.0 ‰, assuming moisture is originating from the Pacific Flank and traversing the Dome to the Inland Flank. Due to elevation differences, the borehole temperature estimate at Core F (Inland) is warmer than Borehole L (Dome). For air masses traversing the Dome Summit to precipitate at Core F (Inland), the temperature would have to be colder in order to condense more water vapor in a given air mass. Therefore, it is possible that air masses originating on the warmer Pacific Flank and contouring the Dome could cause snow deposition at Core F (Inland). However, this does not explain the differing temperature regimes nor the full difference in δD values. Furthermore, low accumulation rates and low δD standard deviation on the Inland Flank suggest that a completely different atmospheric circulation pattern is affecting the Inland Flank.

4.4 Deuterium excess

XS is highest at Core E (Pacific) and lowest at Core F (Inland). The overall trend in XS decreases from the Pacific Flank to the Inland Flank with a linear regression R2 value of 0.73. Dome Summit shallow ice core XS measurements do not fully agree between Cores D, C, and B. Specifically, Core B (Dome) shows an XS value of 4.8 ‰, whereas Core D (Dome) and Core C (Dome) have XS values of 2.8 and 3.2 ‰, respectively. This discrepancy may be caused by converging ASL-La Niña and ASL-El Niño signals on the Dome Summit, causing chaotic variations in XS over short distances between Cores D, C, and B.

CPD
9, 2681–2715, 2013

The north–south decrease in XS is best explained by the strength of the ASL. During La Niña, the ASL circulation is strongest, which could pull atmospheric water vapor from more distant and warmer SST source regions. During El Niño, the ASL circulation is weakest, which could pull moisture from less distant and colder SST source regions. The overall XS trend indicates warmer moisture source SSTs for ice cores towards the Pacific Flank, and colder moisture source SSTs for ice cores towards the Inland Flank (Fig. 10).

5 Discussion

5.1 Microclimate

Siple Dome isotopic values appear to be related to the location of the ASL in relation to ENSO (Fig. 11). Specifically, the Pacific Flank and the Dome Summit are subject to a direct warm air mass from the Ross Sea during the ASL-La Niña mode (Bertler et al., 2006; Nicolas and Bromwich, 2011). Over the time period studied (1920–1995), ASL-La Niña warm air masses likely cause increased borehole temperature measurements in Borehole L (Dome) and Borehole G2 (Pacific), in addition to heavier isotopic values (warmer signal) on the Dome Summit and Pacific Flank. The increased strength of the ASL during La Niña may pull air masses from more geographically diverse and distant locations with warmer SSTs, which is evident in increased XS values towards the Pacific Flank. Conversely, the Inland Flank is subject to a less direct influx of cold air flowing downslope towards the Ross Ice Shelf during ASL-El Niño events associated with strong katabatic winds (Bromwich et al., 1993; Bertler et al., 2006). This cold air mass likely causes Borehole H (Inland) and Borehole J (Inland 32 km S) to follow a colder temperature profile than the Dome Summit and Pacific Flank, which is evident in depleted isotopic values (colder signal) on the Inland Flank. The decreased strength of the ASL during El Niño may pull more local polar air masses originating from colder SST regions, which is evident in decreased XS values towards the Inland Flank.

CPD
9, 2681–2715, 2013

In a broader framework, Siple Dome isotopic values can be related to temperature gradients between the ice core moisture source and final ice core deposition area, where larger temperature gradients from source to deposition will result in greater isotopic depletion. Moisture deposition in the deep Siple Dome ice core has been shown to be sourced in the mid-latitude South Pacific (Schilla, 2007). Based on this source region, Siple Dome shallow ice core isotopic values can be explained in two ways:

1. ASL-La Niña direct (ocean to land) warm air masses result in a smaller temperature gradient from source (generally warm sub-tropical ocean SST regions) to deposition (warm ASL-La Niña air mass), resulting in enriched (heavier) isotopes and higher XS values on the Pacific Flank and Dome Summit. Conversely, more local ASL-El Niño indirect air masses (ocean to land plus inland transport) experience much colder surface temperature anomalies over inland Antarctica, which results in a larger temperature gradient from source (less warm polar ocean SST regions) to deposition (cold ASL-El Niño air mass), resulting in isotopes relatively depleted (lighter) and lower XS values on the Inland Flank.

2. SSTs in Siple Dome moisture source regions of the mid-latitude South Pacific have been shown to be anti-correlated with SSTs in the central and east central equatorial Pacific Ocean (where ENSO is defined) (Schilla, 2007). This is consistent with our comparison between the DJFM SOI and δD_B, which shows that depleted (colder) δD_B values are anti-correlated with ENSO cold events, and vice versa. Therefore, during La Niña ENSO events (cold tropical SSTs), mid-latitude SSTs are warm, causing smaller source-to-deposition temperature gradients and enriched isotopic signals in δD_B. The opposite occurs during El Niño.

These counterintuitive effects help explain the inverse relationship between the DJFM SOI and δD_B values, as well as ASL-ENSO moisture signals. Overall, the weight of evidence shows that Siple Dome is experiencing two distinct climatic signals superimposed on an ENSO signal, where warm air masses during the ASL-La Niña mode originating from warmer SST regions tend to influence the Pacific Flank and Dome

CPD
9, 2681–2715, 2013

Summit, and cold air masses during the ASL-El Niño mode originating from colder SST regions, and associated with strong katabatic winds, tend to influence the Inland Flank. The microclimate effect results in north-south gradients of accumulation, standard deviation, and XS; two distinct warm and cold borehole temperature profiles; discrepancies in δD values compared with temperature and elevation; and a general disagreement in shallow core δD records from 1920–1995. These effects occur over only 60 km on a relatively flat dome (maximum slope of 7.2 m km^{-1}).

5.2 Temporal comparisons to ENSO

Siple Dome's location adjacent to a region of the Southern Ocean with strong atmospheric variability places paleo-ENSO reconstruction in special context. We find that while tropical ocean-atmosphere reorganizations and ENSO itself are detectable at Siple Dome, considerable uncertainty is introduced into ENSO reconstruction due to variations in the ASL. Specifically, the isotopic record is susceptible to a number of spatial and temporal conditions that could alter true tropical-ENSO detection, including (1) ASL-ENSO driven microclimate effects, (2) changes in the strength and dynamics of the ASL (Kreutz et al., 2000), (3) changes in the ENSO system itself (Turner, 2004), (4) changes in other climate oscillations that interact with ENSO, such as the Southern Annular Mode (Fogt and Bromwich, 2006) or Pacific Decadal Oscillation (Gregory and Noone, 2008), (5) wind blown dispersal, such as West Antarctic katabatic winds that transport isotopically depleted inland snow towards the coast (Bromwich et al., 1993), and (6) migration of the Dome over time (Schilla, 2007). Changes in any of these parameters in relation to the others will likely cause non-linear changes in the isotopic record.

Due to the observed microclimate effect, the Siple Dome deep ice core should be interpreted as a mixture of climate signals that may have changed over time, potentially complicating any climate interpretation. While the water isotopes still contain information about ENSO, that information is best viewed as the ENSO modulation of West Antarctic climate, and not strictly of ENSO itself. More importantly, our results show

CPD
9, 2681–2715, 2013

that ice core climate reconstructions from coastal domes in West Antarctica should be carefully considered. For example, it may be useful to recover shallow ice cores from an evenly spaced grid surrounding a deep ice core to validate the coherence of isotopic records. The shallow core records can then compared with atmospheric circulation models (e.g. back trajectory analysis, etc.) to determine a working model for interpreting deep ice core water isotopes and their relevance to synoptic climate reconstructions. If the shallow cores exhibit high variability, it may also be necessary to drill more than one deep ice core (i.e. on both flanks and the dome summit) to capture the full extent of climate variability in the past.

6 Conclusion

Analysis of seven shallow ice cores spanning a 60 km north-south transect of Siple Dome have been analyzed for an El Niño Southern Oscillation (ENSO) signal. Multiple statistical analysis methods of shallow Core B, which is located in the same location as the Siple Dome deep ice core, confirm that paleoclimate reconstruction can offer important insight into the ENSO phenomenon. Specifically, δD_B detects spectral power across the full 2–7 yr ENSO band, captures large-scale ocean atmosphere changes originating in the tropical Pacific Ocean, and approximates the SOI over certain time periods.

However, the combined analysis of borehole temperatures, water isotopes, and accumulation rates reveal the impact of microclimates at Siple Dome related to the modulation of the Amundsen Sea Low Pressure Area (ASL) by ENSO. We find that Siple Dome has two distinct temperature profiles, including a warmer temperature regime on the Pacific Flank and Dome Summit, and a colder temperature regime on the Inland Flank. Water isotope analysis of Core B reveals a heavier isotope signal than borehole temperatures and elevation would predict, likely resulting from warm marine air intrusions coinciding with low pressure centered in the Ross Sea during La Niña events. Overall, the ASL-La Niña mode appears to more greatly influence the Pacific Flank

CPD
9, 2681–2715, 2013

and Dome Summit, whereas the ASL-El Niño mode more greatly influences the Inland Flank.

Due to the complexity of climate in the region, our findings suggest caution in interpreting water isotope signals in West Antarctic ice cores as ENSO. We recommend continued research to understand the dynamics between ASL, ENSO and other climate oscillations in the West Antarctic area. As ASL-ENSO dynamics become better understood, reconstructions of climate will be more useful.

Acknowledgements. The Siple Dome ice core is part of the WAISCORES project with funding from the National Science Foundation Office of Polar Programs West Antarctic Ice Sheet (WAIS) initiative. The WAISCORES website can be accessed at http://nsidc.org/data/waiscores/data.html and offers permanently archived WAISCORES data and project information.

References

Alley, R.: Visible Stratigraphic Dating, Siple Dome and Upstream C Cores, available at: http://nsidc.org/api/metadata?id=nsidc-0121, National Snow and Ice Data Center, Boulder, Colorado, USA, 2003. 2687

Bertler, N. A. N., Barrett, P. J., Mayewski, P. A., Fogt, R. L., Kreutz, K. J., and Shulmeister, J.: El Niño suppresses Antarctic warming, Geophys. Res. Lett., 31, L15207, doi:10.1029/2004GL020749, 2004. 2683

Bertler, N. A. N., Naish, T. R., Mayewski, P. A., and Barrett, P. J.: Opposing oceanic and atmospheric ENSO influences on the Ross Sea Region, Antarctica, Adv. Geosci., 6, 83–86, doi:10.5194/adgeo-6-83-2006, 2006. 2683, 2684, 2694, 2705

Blunier, T., Chappellaz, J., Schwander, J., Dallenbach, A., Stauffer, B., Stocker, T. F., Raynaud, D., Jouzel, J., Clausen, H. B., Hammer, C. U., and Johnsen, S. J.: Asynchrony of Antarctic and Greenland climate change during the last glacial period, Nature, 394, 739–743, 1998. 2686

Bromwich, D. H., Carrasco, J. F., Liu, Z., and Tzeng, R.-Y.: Hemispheric atmospheric variations and oceanographic impacts associated with katabatic surges across the ross ice shelf, Antarctica, J. Geophys. Res., 98, 13045–13062, 1993. 2684, 2686, 2694, 2696

CPD
9, 2681–2715, 2013

Bromwich, D. H., Rogers, A., Kållberg, P., Cullather, R., White, J., and Kreutz, K.: ECMWF analyses and reanalyses depiction of ENSO signal in Antarctic precipitation, J. Climate, 13, 1406–1420, 2000. 2683, 2684

Bromwich, D. H., Monaghan, A., and Guo, Z.: Modeling the ENSO modulation of Antarctic climate in the late 1990s with the polar MM5, J. Climate, 17, 109–132, 2004. 2683

Carleton, A. M.: Atmospheric teleconnections involving the Southern Ocean, J. Geophys. Res., 108, 8080, doi:10.1029/2000JC000379, 2003. 2684

Clow, G.: Siple Dome Shallow Ice Core Borehole Measurements, National Snow and Ice Data Center, Boulder, Colorado, USA, 1996. 2687

Cuffey, K. M. and Steig, E. J.: Isotopic diffusion in polar firn: implications for interpretation of seasonal climate parameters in ice-core records, with emphasis on central Greenland, J. Glaciol., 44, 273–284, 1998. 2689

Cullather, R. I., Bromwich, D. H., and VanWoert, M. L.: Interannual variations in Antarctic precipitation related to El Niño southern oscillation, J. Geophys. Res.-Atmos., 101, 19109–19118, 1996. 2683, 2684

Dansgaard, W.: Stable Isotopes in Precipitation, Tellus, 16, 436–468, 1964. 2685

Delaygue, G., Masson, V., Jouzel, J., Koster, R. D., and Healy, R. J.: The origin of Antarctic precipitation: a modelling approach, Tellus B, 52, 19–36, 2000. 2683

Diaz, H. F., Hoerling, M. P., and Eischeid, J. K.: ENSO variability, teleconnections and climate change, Int. J. Climatol., 21, 1845–1862, 2001. 2683

Dunbar, R. B., Wellington, G. M., Colgan, M. W., and Glynn, P. W.: Eastern Pacific Sea surface temperature since 1600 A. D.: the delta-^{18}O record of climate variability in galapagos corals, Paleoceanography, 9, 291–315, 1994. 2689

Epstein, S. and Mayeda, T.: Variation of O-18 content of waters from natural sources, Geochim. Cosmochim. Acta, 4, 213–224, 1953. 2687

Fogt, R. L. and Bromwich, D. H.: Decadal variability of the ENSO teleconnection to the high-latitude South Pacific governed by coupling with the southern annular mode, J. Climate, 19, 979–997, 2006. 2696

Ghil, M., Allen, M. R., Dettinger, M. D., Ide, K., Kondrashov, D., Mann, M. E., Robertson, A. W., Saunders, A., Tian, Y., Varadi, F., and Yiou, P.: Advanced spectral methods for climatic time series, Rev. Geophys., 40, 1003, 2002. 2688

CPD
9, 2681–2715, 2013

Gregory, S. and Noone, D.: Variability in the teleconnection between the El Niño Southern Oscillation and West Antarctic climate deduced from West Antarctic ice core isotope records, J. Geophys. Res., 113, D17110, doi:10.1029/2007JD009107, 2008. 2696
Guo, Z., Bromwich, D., and Hines, K.: Modeled Antarctic precipitation, Part II: ENSO modulation over West Antarctica, J. Climate, 17, 448–465, 2004. 2683
Hendricks, M. B., DePaolo, D. J., and Cohen, R. C.: Space and time variation of δ^{18}O and δD in precipitation: can paleotemperatnre be estimated from ice cores?, Global Biogeochem. Cy., 14, 851–861, 2000. 2686
Jacobel, R. W. D. C. and Harner, A.: Ice velocities near a relict flow feature on siple dome, Antarctic J. US, 29, 62–66, 1994.
Jouzel, J. and Merlivat, L.: Deuterium and O-18 in precipitation – modeling of the isotopic effect during snow formation, J. Geophys. Res.-Atmos., 89, 1749–1757, 1984. 2686
Jouzel, J., Vimeux, F., Caillon, N., Delaygue, G., Hoffmann, G., Masson-Delmotte, V., and Parrenin, F.: Magnitude of isotope/temperature scaling for interpretation of central Antarctic ice cores, J. Geophys. Res.-Atmos., 108, 4361, doi:10.1029/2002JD002677, 2003. 2686
Kavanaugh, J. L. and Cuffey, K. M.: Space and time variation of δ^{18}O and δD in Antarctic precipitation revisited, Global Biogeochem. Cy., 17, 10–17, 2003. 2686
Kreutz, K. J., Mayewski, P. A., Pittalwala, I. I., Meeker, L. D., Twickler, M. S., and Whitlow, S. I.: Sea level pressure variability in the Amundsen Sea region inferred from a West Antarctic glaciochemical record, J. Geophys. Res.-Atmos., 105, 4047–4059, 2000. 2696
Lamorey, G. W.: Siple Shallow Core Density Data, available at: http://nsidc.org/api/metadata?id=nsidc-0129, National Snow and Ice Data Center, Boulder, Colorado, USA, 2003. 2687
Markle, B. R., Bertler, N. A. N., Sinclair, K. E., and Sneed, S. B.: Synoptic variability in the Ross Sea Region, Antarctica, as seen from back-trajectory modeling and ice core analysis, J. Geophys. Res.-Atmos., 117, D02113, doi:10.1029/2011JD016437, 2012. 2683
Masson-Delmotte, V., Hou, S., Ekaykin, A., Jouzel, J., Aristarain, A., Bernardo, R. T., Bromwich, D., Cattani, O., Delmotte, M., Falourd, S., Frezzotti, M., Gallée, H., Genoni, L., Isaksson, E., Landais, A., Helsen, M. M., Hoffmann, G., Lopez, J., Morgan, V., Motoyama, H., Noone, D., Oerter, H., Petit, J. R., Royer, A., Uemura, R., Schmidt, G. A., Schlosser, E., Simões, J. C., Steig, E. J., Stenni, B., Stievenard, M., van den Broeke, M. R., van de Wal, R. S. W., van de Berg, W. J., Vimeux, F., and White, J. W. C.: A review of Antarctic surface snow isotopic composition: observations, atmospheric circulation, and isotopic modeling, J. Climate, 21, 3359–3387, 2008. 2686, 2692

CPD
9, 2681–2715, 2013

Meyerson, E. A., Mayewski, P. A., Kreutz, K. J., Meeker, L. D., Whitlow, S. I., and Twickler, M. S.: The polar expression of ENSO and sea-ice variability as recorded in a South Pole ice core, Ann. Glaciol., 35, 430–436, 2002. 2684

Nicolas, J. P. and Bromwich, D. H.: Climate of West Antarctica and influence of marine air intrusions, J. Climate, 24, 49–67, 2011. 2683, 2694

Noone, D. and Simmonds, I.: Annular variations in moisture transport mechanisms and the abundance of δ^{18}O in Antarctic snow, J. Geophys. Res.-Atmos., 107, 4742, doi:10.1029/2002JD002262, 2002. 2686

Percival, D. B. and Walden, A. T.: Spectral analysis for physical applications: multitaper and conventional univariate techniques, available at: http://www.loc.gov/catdir/toc/cam021/92045862.html, Cambridge University Press, Cambridge, New York, N. Y., USA, 1993. 2688

Petit, J., White, J., Young, N., Jouzel, J., and Korotkevich, Y.: Deuterium excess in recent Antarctic snow, J. Geophys. Res., 96, 5113–5122, 1991. 2686

Schilla, A. S.: The stable isotopes and deuterium excess from the Siple Dome ice core: implications for the late Quaternary climate and elevation history of the Ross Sea Region, West Antarctica, Book, microform, online, University of Colorado, 2007. 2695, 2696

Schneider, D., Steig, E., and Comiso, J.: Recent climate variability in Antarctica from satellite-derived temperature data, J. Climate, 17, 1569–1583, 2004. 2683

Shimizu, H.: Glaciological studies in West Antarctica, 1960–1962, Antarct. Snow Ice Stud., 2, 37–64, 1964. 2692

Steig, E. J. and White, J. W. C.: Siple Dome highlights: Stable isotopes, National Snow and Ice Data Center, Boulder, Colorado, USA, 2003. 2687

Thomson, D. J.: Spectrum estimation and harmonic analysis, available at: http://ieeexplore.ieee.org/xpls/abs_all.jsp?arnumber=1456701, Proc. IEEE, 70, 1055–1096, 1982. 2688

Torrence, C. and Compo, G.: A practical guide to wavelet analysis, B. Am. Meteorol. Soc., 79, 61–78, 1998. 2688

Trenberth, K. E. and Hoar, T. J.: El Niño and climate change, Geophys. Res. Lett., 24, 3057–3060, 1997. 2683

Turner, J.: The El Niño-Southern oscillation and Antarctica, Int. J. Climatol., 24, 1–31, 2004. 2683, 2696

Urban, F. E., Cole, J. E., and Overpeck, J. T.: Influence of mean climate change on climate variability from a 155-year tropical Pacific coral record, Nature, 407, 989–993, 2000. 2690

CPD
9, 2681–2715, 2013

Vaughn, B. H., White, J. W. C., Delmotte, M., Trolier, M., Cattani, O., and Stievenard, M.: An automated system for hydrogen isotope analysis of water, Chem. Geol., 152, 309–319, 1998. 2687

CPD
9, 2681–2715, 2013

Table 1. Siple Dome ice core sites (B–H) and borehole temperature measurement sites (G, L, H, J) used in this study.

Site	Data type	Latitude (degrees)	Longitude (degrees)	Length of ice Rrcord (yrs)	Bottom depth (m)
E	Ice	81°18.14′ S	148°18.14′ W	1908–1995	20.0
G	Ice/Temp	81°34.25′ S	148°35.85′ W	1917–1995	20.0
D	Ice	81°38.73′ S	148°47.16′ W	1901–1995	20.0
C	Ice	81°39.30′ S	148°47.66′ W	1836–1995	30.0
B	Ice	81°39.53′ S	148°48.72′ W	1657–1995	54.0
L	Temp	81°39.53′ S	148°48.72′ W		
H	Ice/Temp	81°44.37′ S	148°58.61′ W	1898–1995	20.0
F	Ice	81°54.51′ S	149°20.22′ W	1872–1995	20.0
J	Temp	81°55.50′ S	149°22.58′ W		

CPD
9, 2681–2715, 2013

Table 2. Siple Dome shallow ice core data summary. The δD, δ^{18}O, XS, accumulation, and δD standard deviation values are averages from 1920–1995.

Site	Grid (km)	Elevation (m a.s.l.)	δD (‰)	δ^{18}O (‰)	XS (‰)	Accumulation (cm yr^{-1} ice eq.)	δD Std. Dev. (‰)	Borehole temp. (°C at 20 m depth)
E	30° N	400	−199.1	−25.6	5.8	11.7	16.0	
G	10° N	590	−202.4	−25.9	5.1	13.4	14.8	−24.79
D	1° N	615	−205.4	−26.1	2.8	11.0	13.9	
C	0°	615	−203.0	−25.8	3.2	11.2	14.1	
B	0.5° S	615	−202.3	−25.9	4.8	11.1	13.9	
L	0.5° S	615						−25.12
H	10° S	590	−207.5	−26.4	3.3	9.3	13.8	−25.33
F	30° S	450	−220.2	−27.8	2.5	8.2	11.19	
J	32° S	435						−24.22

CPD
9, 2681–2715, 2013

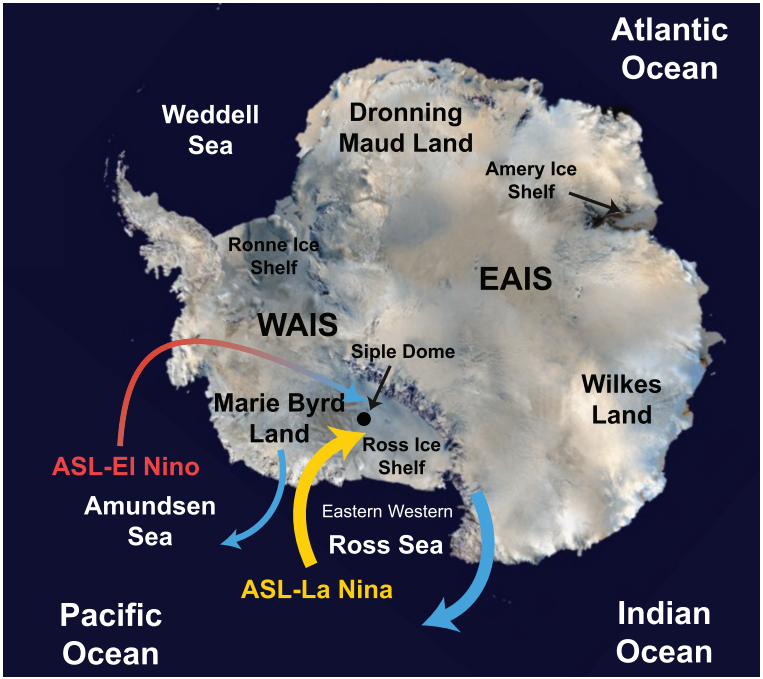

Fig. 1. Map of Antarctica showing variations in the Amundsen Sea Low Pressure Area (ASL). The ASL circulation has been shown to shift from the Ross Sea to the Amundsen Sea during La Niña and El Niño conditions, respectively (Bertler et al., 2006). The size of the arrows represent the strength of the ASL. The orange arrow represents a warm air mass, the red arrow represents a comparatively warmer air mass, and blue arrows represent cold air masses. Modified after Bertler et al. (2006).

CPD
9, 2681–2715, 2013

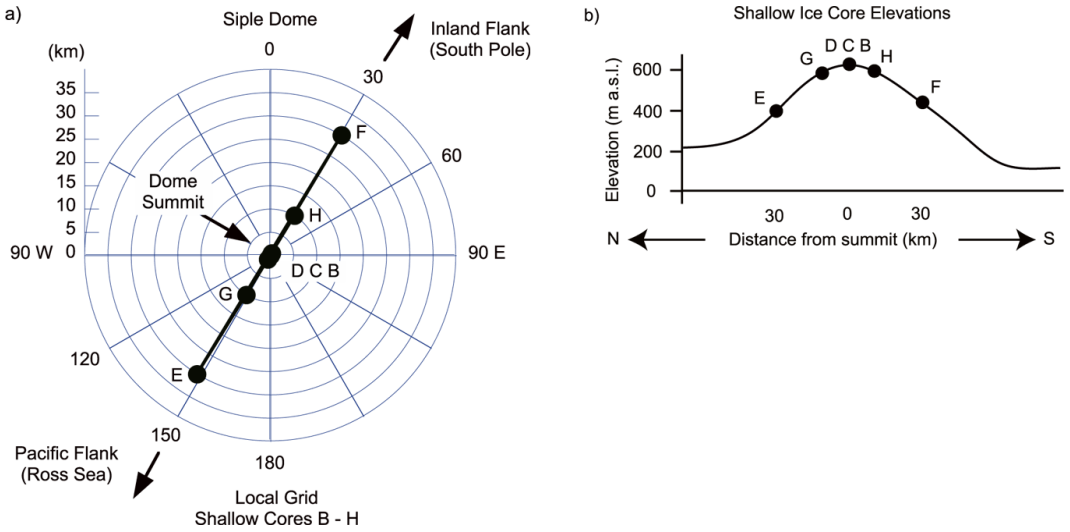

Fig. 2. (a) Local map of Siple Dome including grid locations of shallow ice cores B–H. The Pacific Flank cores are to the North of the Dome Summit, and the Inland Flank cores are to the South of the Dome Summit. **(b)** Cross section of Siple Dome.

CPD
9, 2681–2715, 2013

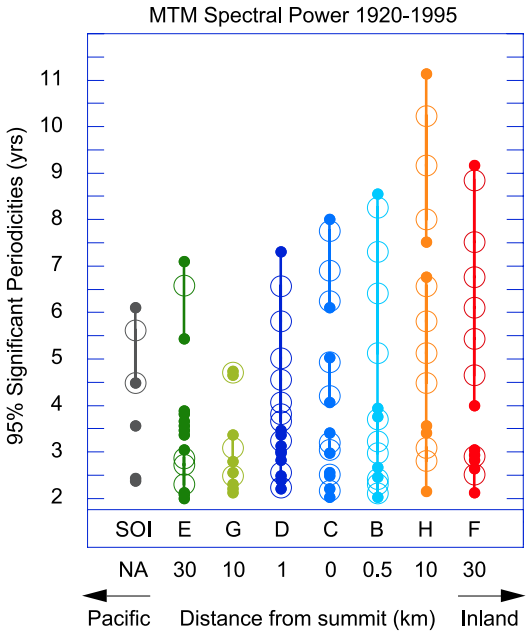

Fig. 3. MTM spectral analysis of Siple Dome shallow ice cores and the DJFM SOI for the years 1920–1995. Solid lines (ending with solid circles) designate 95 % significance periodicities relative to an estimated red noise background. Open circles denote the location of spectral peaks. Significant periods below 2 yr are not shown due to signal loss from diffusional processes in the firn.

CPD
9, 2681–2715, 2013

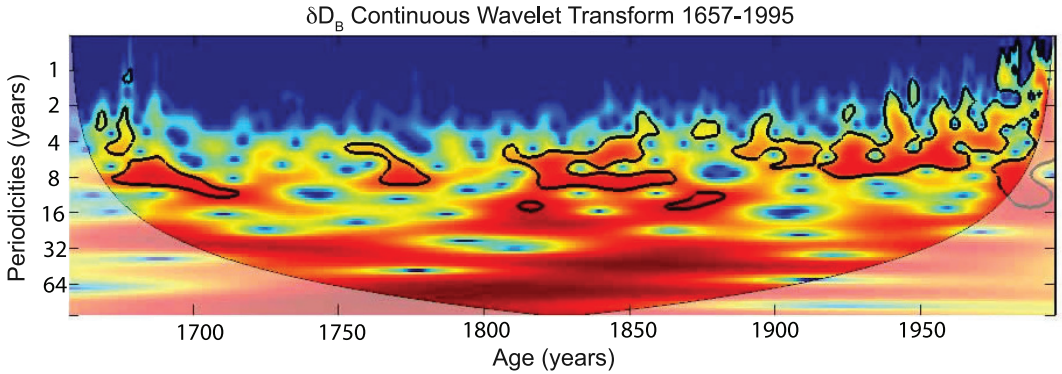

Fig. 4. Continuous Wavelet Transform (CWT) for δD_B. The CWT expands the time series into time frequency space. Red regions represent the regions of highest spectral power, and blue regions represent the regions of lowest spectral power. The semi-transparent white regions designate areas where edge effects distort the wavelet signal. Black contours enclose areas of 95 % statistical significant periodicities in the ice core record relative to an estimated red noise background.

CPD
9, 2681–2715, 2013

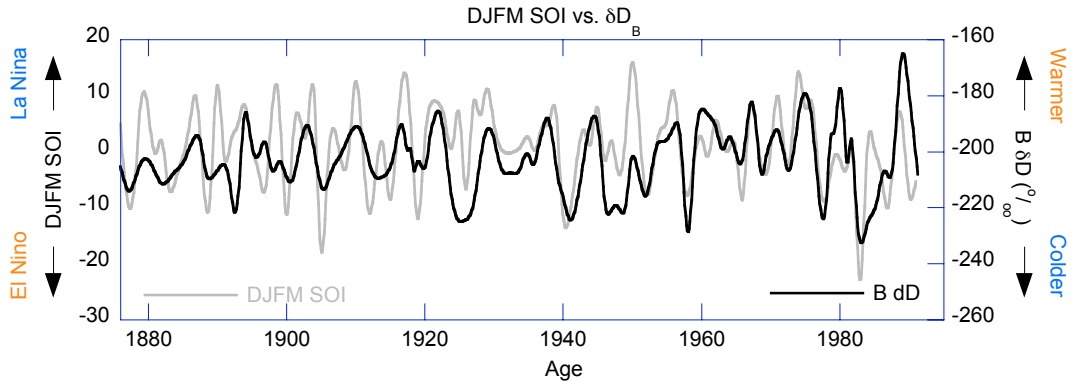

Fig. 5. Core B δD_B (black line) and DJFM SOI (grey line), where δD_B has been re-dated within dating uncertainty limits to the DJFM SOI (±3.5 yr, ~4 % error).

CPD
9, 2681–2715, 2013

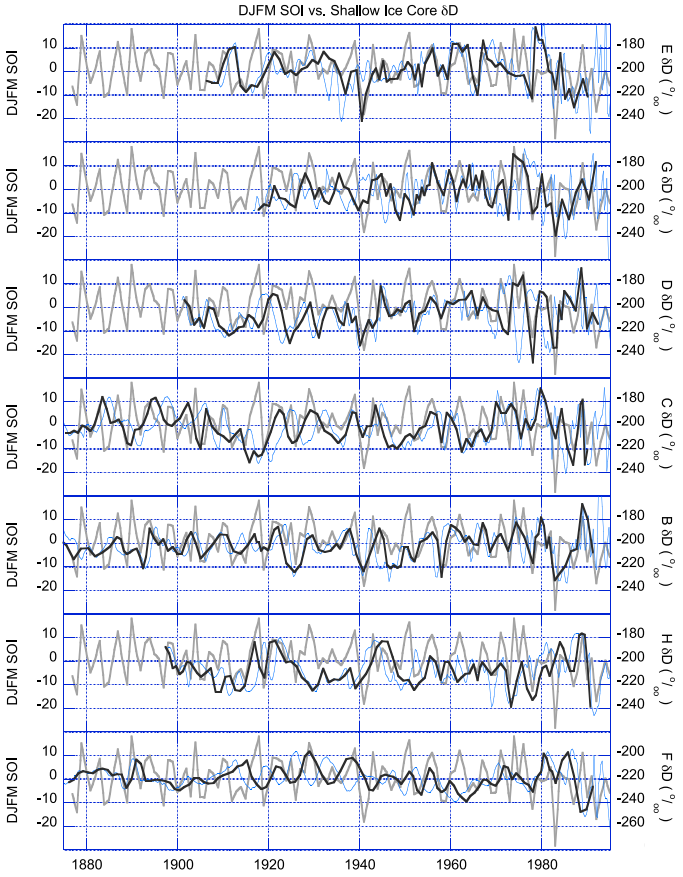

Fig. 6. Siple Dome shallow ice core δD re-dated to DJFM SOI (black line), original δD (blue line), and DJFM SOI (grey line), where the δD re-dated values are within dating uncertainty limits. Note that Core F has a different y-axis range.

CPD
9, 2681–2715, 2013

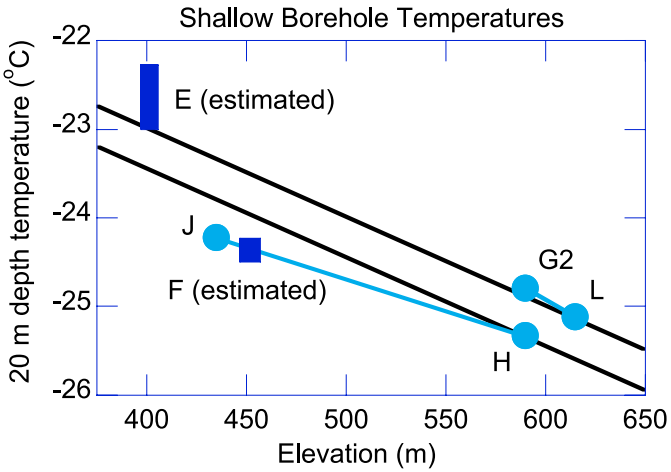

Fig. 7. Shallow 20 m borehole temperatures recorded at Siple Dome. Light blue circles denote temperature measurements. Light blue lines designate temperature trends. Black lines designate adiabats (0.82 °C/100 m) generated from the temperature measurements. No borehole temperatures were taken at Core E or Core F. These temperature values (dark blue rectangles) are estimated using adiabats and temperature trends.

CPD
9, 2681–2715, 2013

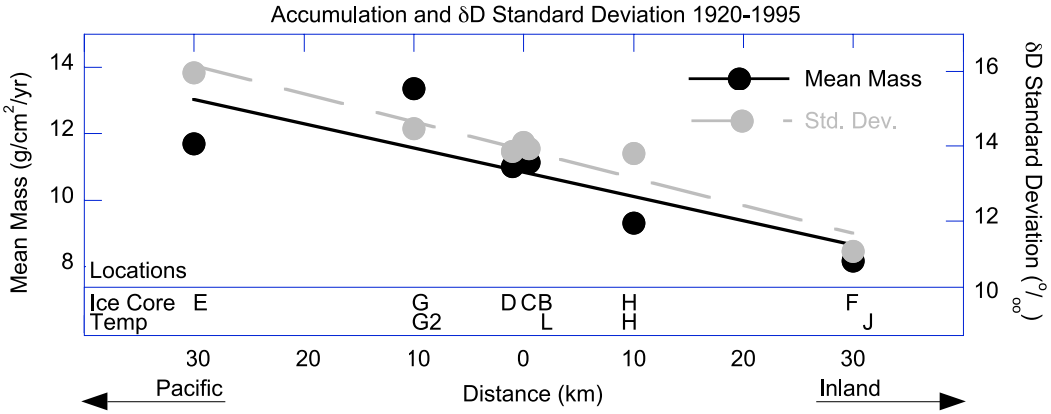

Fig. 8. Shallow ice core mean accumulation (black line) and δD standard deviation (grey line) on Siple Dome. Locations of shallow ice cores and borehole temperature measurements are shown at the bottom of the graph.

CPD
9, 2681–2715, 2013

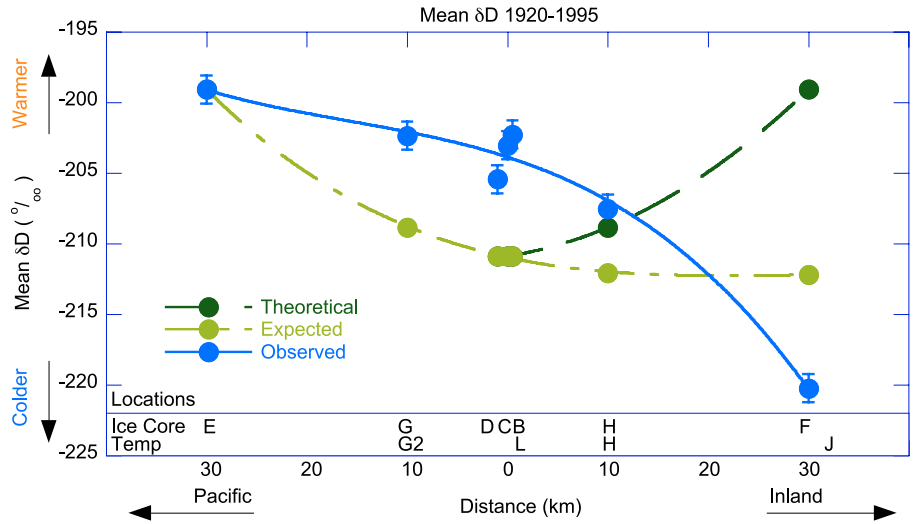

Fig. 9. Shallow ice core mean δD on Siple Dome. The light blue dots denote observed mean isotopic values (error bars attached) and the light blue line shows the observed isotopic trend. The light green line depicts predicted mean isotopic values using shallow borehole temperatures and elevations, and assumes Core E is the first location on Siple Dome to receive precipitation. Since no borehole temperature was taken at Core E, the local adiabat from Borehole G2 and Borehole L is used to generate a predicted mean isotopic value. The dark green line depicts theoretical mean isotopic values if moisture was converging on Siple Dome uniformly from both the Pacific and Inland Flanks. Locations of shallow ice cores and borehole temperature measurements are shown at the bottom of the graph.

CPD
9, 2681–2715, 2013

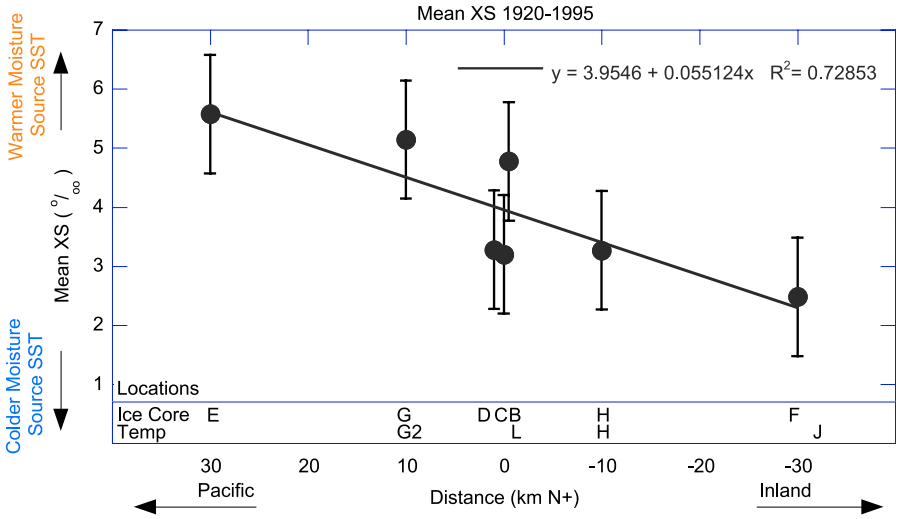

Fig. 10. Shallow ice core mean XS on Siple Dome. The solid dots denote observed mean XS values (uncertainty bars attached). Locations of shallow ice cores and borehole temperature measurements are shown at the bottom of the graph.

CPD
9, 2681–2715, 2013

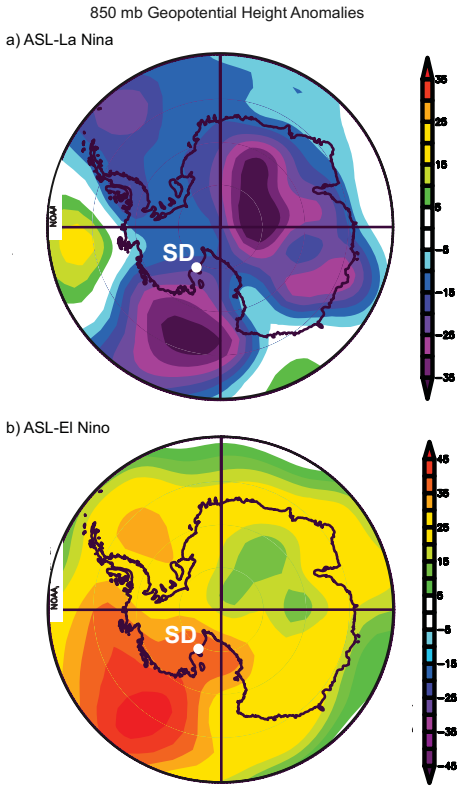

Fig. 11. 850 mb geopotential height anomalies relative to a 1981–2010 base period associated with **(a)** December to January values of the SOI greater than or equal to 90 % (i.e. strong La Niña years; 1962, 1974, 1976, 2008, 2011, 2012) and **(b)** December to January values of the SOI less than or equal to 10 % (i.e. strong El Niño years; 1958, 1983, 1987, 1992, 1998, 2010). The low pressure system strengthens during La Niña events and weakens during El Niño events. The white dot is Siple Dome (SD).

CPD
9, 2681–2715, 2013